Fourier Theory in the Analysis of Sound

Joseph Pritchard - Adelaide University

November 8, 2019

1 Introduction

The mathematics underpinning sound waves was greatly progressed in 1807 by Jean Fourier [1] and his development of the Fourier transform, which provided key insights into how sound and other waves behave. The onset of the computer revolution produced a great many ways to test and utilize these theories. Through the use of virtual instruments - a physical measurement tool in tandem with computer software - we showcase the versatility of Fourier theory on numerous wave sources, both natural and electronic, whilst demonstrating several optimal experimental techniques.

2 Equipment Preparation

An output channel of a digital Oscilloscope is connected to the input port of a computer, allowing data from the oscilloscope display to be accessed and analyzed using computer software with MATLAB and fast Fourier transform (FFT) functionality. A signal generator is present with the ability to produce sine, square and triangular waves over a large frequency domain. For our purposes this is used within the range $100Hz < f < 1.2kHz$. A coaxial cable is used to connect the output of the signal generator to the input of the oscilloscope, allowing for the digital display of the produced waveform.

For the detection of sound waves, a microphone is present. Due to the general small voltage amplitude of sound signals detected by the microphone an amplifier is connected in tandem, allowing for the amplification of small signals $V < 10mV$. A coaxial cable is connected to the output of the amplifier

which can again be connected to the input of the digital oscilloscope, allowing for the presentation of sound wave signals on the oscilloscope screen.

3 Optimization of FFT Display Method

3.1 Sampling Interval

To ensure correct calibration of equipment the relationship between software input commands and oscilloscope behavior is confirmed. The sampling interval is specified within the MATLAB computer software and the resulting data is plotted in time, again in MATLAB, for two sampling intervals. To give clear perception into the correlation, sampling intervals of moderate spacing are selected, one at $20\mu s$ and one at $40\mu s$.

3.2 Graphical Interpretation

It is important to note the ease with which insight is gained from the results relies heavily on the choice of axis scalings. To this effect, a $1kHz$ sine wave is produced and it's time signal data then recorded in the MATLAB software. MATLAB is then used to convert the signal to frequency space via a fast Fourier transform. The resulting data is then plotted using loglog, semilogy and liner axis which are then cross compared with one another. The most easily interpreted scaling is chosen and used hereafter.

3.3 Discontinuity Analysis

In creating a Fourier transform, the MATLAB script first repeats the collected time data end to end iteratively. As such discontinuities between the start and end points of the time samples can lead to unrealistic results, the effect of which is now examined.

To allow for a larger data set to be gathered the signal generator frequency is now set to $1kHz$, while the sampling frequency is maintained at $20\mu s$. MATLAB software produces a stitching of the last and first 50 data points recorded by the oscilloscope, allowing for a precise determination of the discontinuity extent. Using this method, signal generator frequency is

incrementally adjusted and the resulting effect on discontinuity size is observed. This process is repeated until the time signal appears relatively smooth. Once this stage is reached the data is then fast Fourier transformed using the MATLAB software to produce a plot of amplitude against frequency.

Frequency is once more adjusted until a point of large discontinuity is attained, characterized by a sudden jump from a minimum to a maximum with infinite slope. This setting can be seen in figure 1.

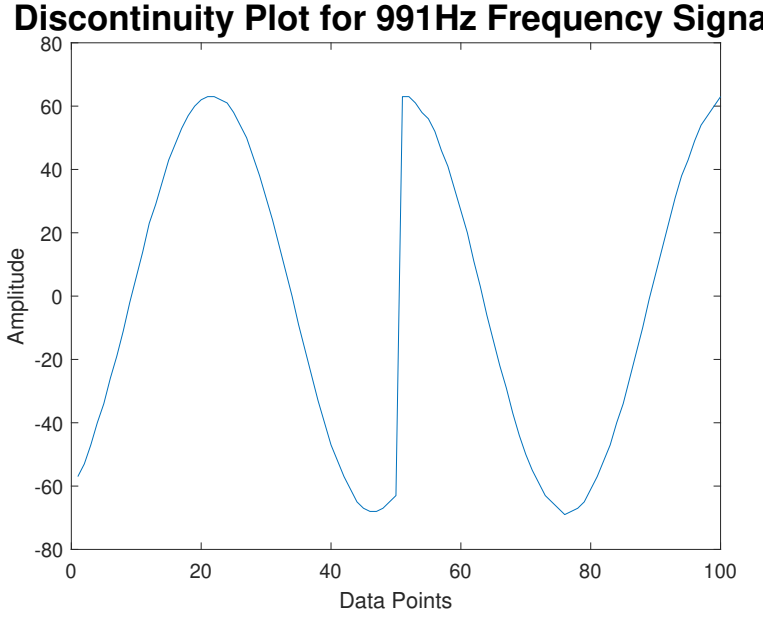

(a) Figure 1

The resulting time signal is again Fourier transformed to display the relative presence of differing frequency components.

The plots produced from both methods are compared to discern the effect of discontinuities on the Fourier transform plot produced.

3.4 Hanning Window

A Hann function on the interval $(0, L)$ is given by [2]

$$cos^2\left(\frac{\pi\,(2x+L)}{2L}\right) \tag{1}$$

To apply a Hanning window to our data set is to take the product of every measured data data point with the corresponding Hann value at that point within the interval [2]. This windowing is readily done in the MATLAB software.

In analyzing the effect of the window function, the maximum discontinuity sine wave found previously is produced by the signal generator. The sampling interval is set to $20\mu s$ to provide sufficient data samples. The generated signal is recorded in the MATLAB software. A script is then used to produce a Hann smoothed data set and the result is displayed in both the time domain as well as the Fourier transformed frequency domain. The displayed data is compared to the purely discontinuous data signal analyzed previously, to judge the relative merits of Hann smoothing.

3.5 Optimal Sampling Rate

The Nyquist Theorem stipulates in order to discern a frequency of f_N within a sample, a sampling frequency at least twice this frequency must be used such that

$$f_s \geq 2f_N \tag{2}$$

where f_s denotes the sampling frequency [3]. Deviations from this critical value are tested by varying f_s above and below this value - over and under sampling. Once again a signal generator frequency of $1kHz$ is used leading to a minimum f_s of $2kHz$. This is converted to a sampling interval size of $500\mu s$, via the relation

$$f_s = T_s^{-1}$$

Due to limitations in the oscilloscope scaling, four frequency samples are collected - two above and two below f_s - at sampling interval sizes of $100\mu s$, $250\mu s$, $500\mu s$, $750\mu s$ and $1ms$. These results are Hann smoothed to remove the effects of discontinuities and plotted in frequency space for comparison.

4 Optimization Results

Adjusting the sampling interval size produces a scaling of the oscilloscope x-axis display and thus stretching of the gathered data, as can be seen in figures 2 and 3.

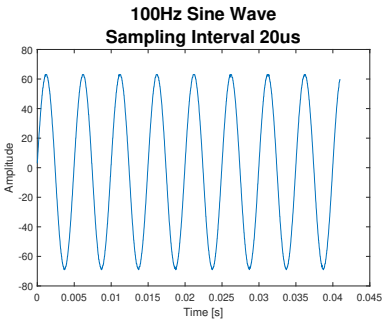

(a) Figure 2

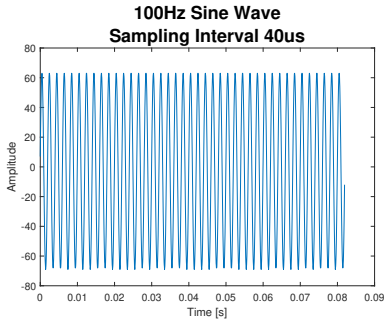

(b) Figure 3

A shorter sampling interval will provide more data for analysis however it is foreseeable too short a sampling interval may prevent the waveform being properly visible by scaling of the display. As such the optimal f_s for the chosen input frequency will be set according to these limits.

It is also noted the Oscilloscope display provides reference for the sampling interval in real time by showing the width per division of the display window. Given there are 2500 points within the display [4] this can be used to find the sampling interval since

$$T_{sampling} = \frac{10\,(SEC/DIV)}{2500} \tag{3}$$

Various axis scalings of frequency space plots in log-log, semi-logy and linear settings are shown in figures 4, 5 and 6.

Note the linear plot scales the results to either end of the display, rendering them unreadable. Similar issues arise with the choice of semi-logy axis as the results are scaled such that a clear interpretation is not possible. To remove both of these issues graphs with axis plotted in log-log format will be used here on out as it is noted this removes all the aforementioned issues.

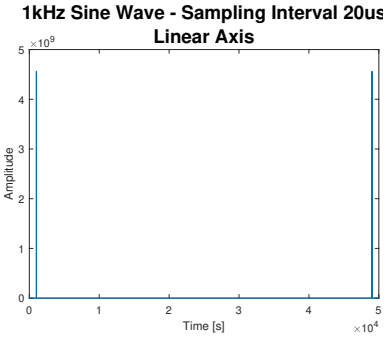

(a) Figure 4

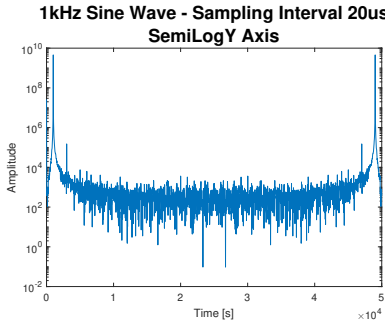

(b) Figure 5

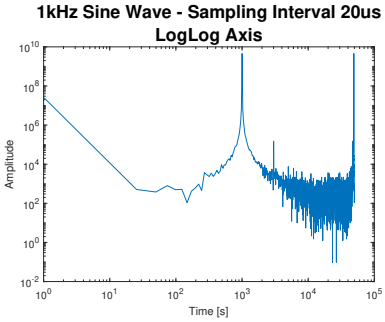

(c) Figure 6

The presence of discontinuities in the time space waveform is found to reduce the clarity of the resulting Fourier transform, as can be seen in comparing the continuous and discontinuous frequency displays of the $1kHz$ sine wave (Figures 7 and 8).

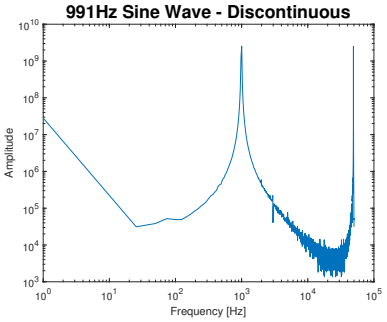

(a) Figure 7

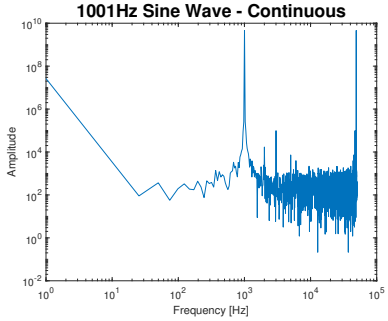

(b) Figure 8

We note the amplitude of low frequencies in the rage $100kHz$ up to $2kHz$ is greatly increased with the added discontinuity rising from 10^3 to 10^5. We also observe an increase in bandwidth of the $1kHz$ frequency where the full

width half maximum is now $200Hz$ as oppose $100Hz$ in the continuous case. We note the higher frequency behavior is also given an increased amplitude. This alteration in display reduces the ease to which frequency signals can be detected and as such such discontinuous affects are carefully prevented with the use of Hann smoothing.

In applying the window function it is found any discontinuity vanishes as the Hann function places the data in a wave packet form with zeros at the start and end of the display (Figure 9) thus providing an effective means of removing the negative effects of discontinuities.

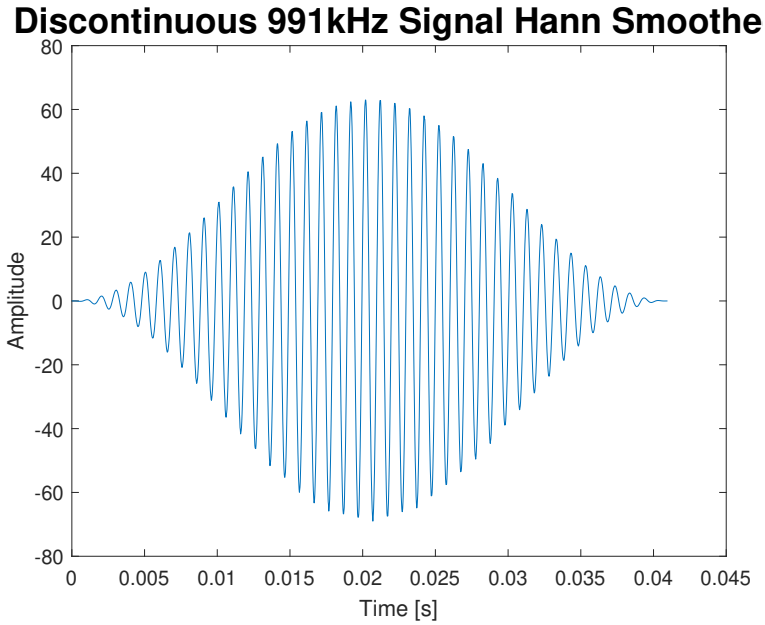

(a) Figure 9

The increase in clarity is further solidified in observation of the frequency displayed data (Figure 10). Note the presence of low amplitude frequencies previously at $10^4 - 10^5$ is now greatly suppressed to a lower level of 10^2, verifying the effectiveness of the Hann window technique. Note also the bandwidth is largely reduced allowing for a more precise measure of the frequency peak location.

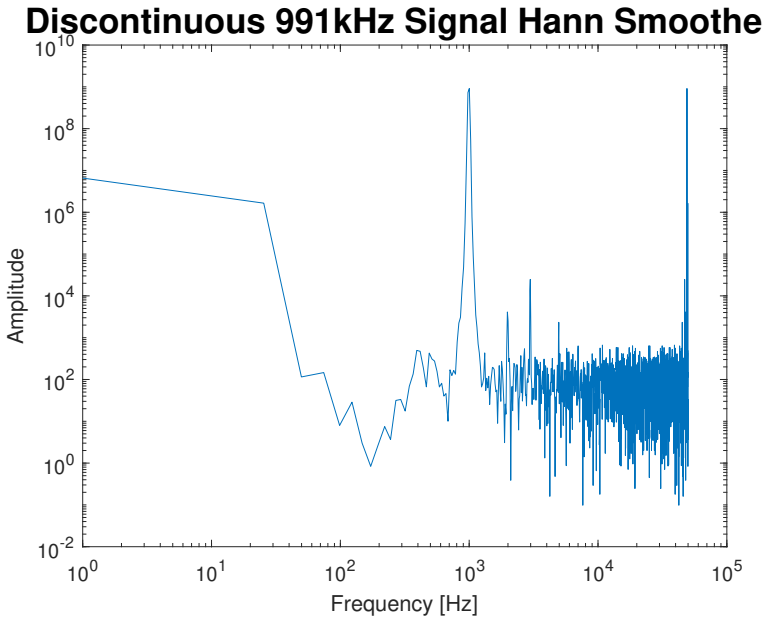

(a) Figure 10

5 Optimization Discussion

In testing the various measurement and analysis techniques the importance of setting optimization in the experimental process was exemplified to a high degree. Without the correct choice of axis scalings the recorded data is not able to be interpreted accurately.

Discontinuities between the start and end of the recorded time signal were found to impact the frequency space results greatly, giving the impression lower frequency signals were abnormally present and increasing the bandwidth of the measured peak, reducing precision. These faults were found to be aptly fixed by the implementation of a Hann window function which removed both of the discontinuity related issues.

6 Complex Wave-forms

6.1 Triangular and Square Wave-forms

The signal generator is set to produce a square wave of $1kHz$ which is then recorded in time space, Hann smoothed and Fourier transformed in the MATLAB software. The same process is performed with a $1kHz$ triangular wave and the two frequency space results are cross compared with each other and the results from the $1kHz$ sine wave measured previously.

6.2 Tuning Forks

The signal generator input cable is now replaced with the input cable of the microphone and amp system to allow for the recording of sound wave-forms. The microphone is then placed facing the Tuning fork amplification chamber opening to ensure clarity of signal. The fork is struck to test equipment detection of signal and ensure scalings are optimally set. Care is taken that the room is silent when striking to remove background effects. A clear signal of the fork sound wave is represented on the oscilloscope by repeatedly striking the fork whilst adjusting the oscilloscope scalings. Once done, the display is frozen on the oscilloscope via the 'time-stop' command. MATLAB software is then used to record the signal in time space and perform a Fourier transform. The resulting plot is analyzed to determine the frequency of the tuning fork. This process is then repeated for a second tuning fork of differing size.

To test mixed signal detection, the microphone is placed adjacent to the amplification chamber openings of both tuning forks simultaneously and both forks are struck at the same time. Oscilloscope screen capture is then taken in the same process as above and the resulting Fourier transform is analyzed.

6.3 Vocals

Fourier techniques are now used to analyze the frequency properties of vocal sounds. The microphone is set up as before and a member of the practical team hums into the microphone. The time space signal produced on the oscilloscope is frozen (via the use of the time-stop command) and the result is captured in the MATLAB software. Most optimal settings found previously

are utilized to ensure the produced signal is clearly presented in the FFT.

The above process is now repeated whilst first recording the members hum on a mobile phone. This recorded signal is then played into the microphone and used to produce an FFT of the digital signal as before.

The two vocal pattern frequency displays are cross compared to determine the relative features of digital against natural voice.

7 Results for Complex Wave-forms

Frequency space results for $1kHz$ square and triangular wave-forms show a high contribution of higher frequency modes as is displayed in Figures 11 and 12.

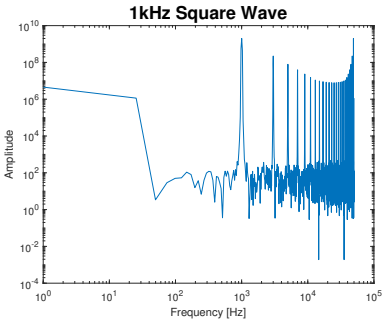

(a) Figure 11

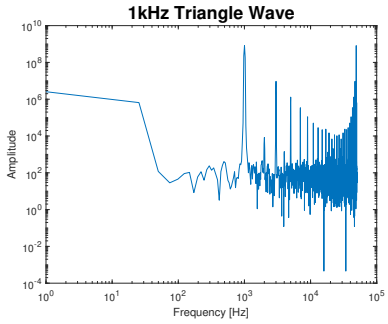

(b) Figure 12

We note the frequency drop of slope is steeper in the case of the triangle wave with the frequencies dropping significantly around the $12kHz$ mark, while for the square wave they pertain with relative consistency dropping only slightly in amplitude. In representing a square and triangular wave as a Fourier series the coefficients are as follows [5]

$$C_{square} \propto \frac{1}{n} \tag{4}$$

and

$$C_{triangle} \propto \frac{1}{n^2} \tag{5}$$

This stipulates higher frequencies should drop off as $\frac{1}{n}$ and $\frac{1}{n^2}$ for the square and triangular wave-forms respectively. Observing our graphs we see this pattern does indeed appear present as the triangle frequency drop off is much more rapid in comparison to that of the square, as is seen in the displayed plots.

Frequency space displays for the tuning forks are shown in figures 13 and 14.

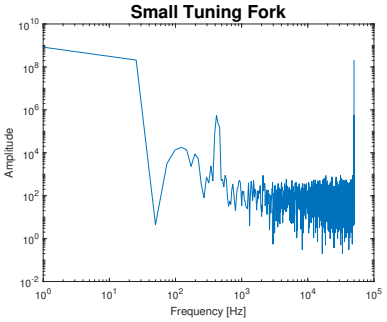

(a) Figure 13

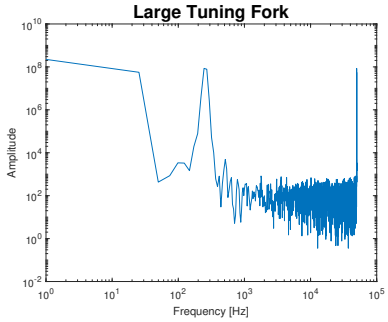

(b) Figure 14

Interpreting the above plots we found the tuning fork frequencies lie close to the $200Hz$ and $400Hz$ marks, with little contribution from frequencies at other levels - outside that which may be attributed to noise. Once struck simultaneously and a Fourier series of the resulting sound wave was taken the resulting frequency spectrum was observed (Figure 15).

We note clear peaks again occur at both the 200 and $400Hz$ frequency markings, attributable to the two independent tuning fork sound waves. This clear signal distinction outlines the strength of the Fourier technique in being able to siphon information from a mixed signal.

In analysis of digital and human voice sound waves the frequency space plots produced are shown in figures 16 and 17. In both cases we note that a low frequency note is present at around 10^2Hz with the additional layering of higher order frequency peaks. For the digital voice case it is noted the lower frequencies are not as prominent as in the natural case. This prominence is likely due to volume limitations on the recording device not present in the natural voice scenario.

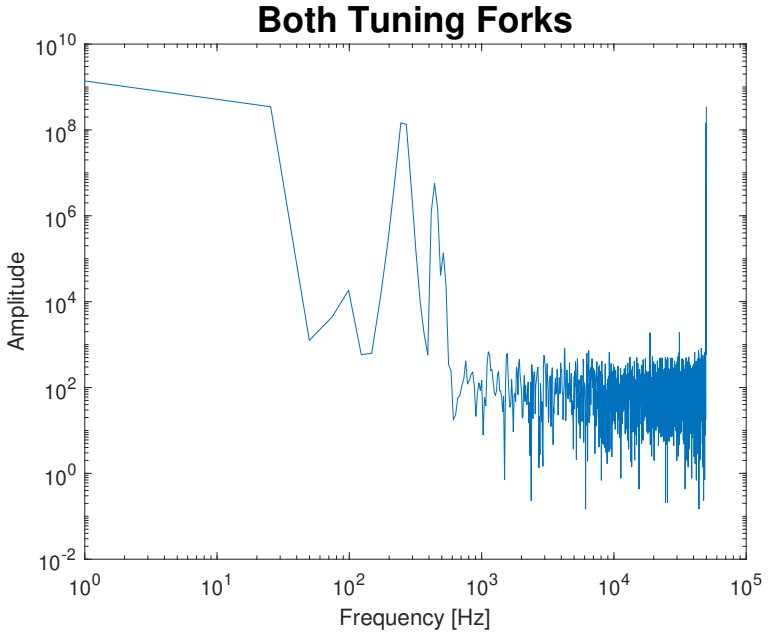

(a) Figure 15

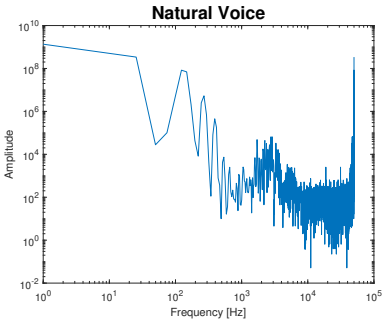

(a) Figure 16

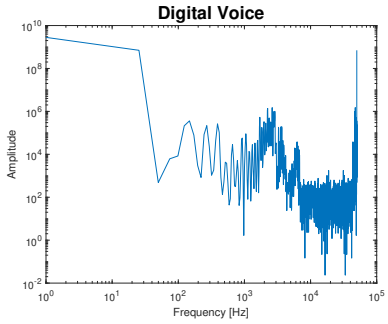

(b) Figure 17

The presence of higher frequencies is aligned with theory as it is known human voice contains layering of higher order frequencies, making it differentiable from a pure sine wave [6].

8 Discussion of Complex Waveforms

In analyzing the frequency domain plots for complex wave-forms and invoking Fourier theory we are able to explain the origin of many physical features present. In the case of triangular and square waves we find a systematic drop-off in amplitudes as frequency increases which are matched well in each case by the predictions of Fourier series theory, outlining the usefulness of the mathematics in explaining the physical processes occurring.

Investigation of tuning forks played both independently and in unison illustrated the ability for a Fourier transform to discern the presence of multiple distinct frequencies in a sound wave signal, with ease of interpretation. This ability was further outlined in the analysis of human voice both natural and digital. Herein Fourier techniques allowed for the identification of higher frequency components. It is important to note that such identification is challenging when simply viewing the time space signal, outlying the power of the Fourier method.

In interpreting complex wave-forms the optimization techniques refined previously were heavily used and greatly increased the ease of interpretation of all of the displayed data.

9 Conclusion

Through the use of Fourier transformation the frequency components of a time space signal can be determined with clarity, allowing for great insight into the nature of both electronic and natural sound waves. The experimental results gathered are found to align heavily with the mathematics developed by Fourier, showcasing the strength of the Fourier technique.

Optimization of experimental and plotting techniques is found to be of great assistance in the interpretation of all the gathered data. The resulting clarity from the appropriate choice of scale settings and Hann smoothing provide results which are readily understood, greatly increasing the effectiveness of all subsequent measurements.

10 Bibliography

[1] Dominguez, A 2016, *Highlights in the history of the Fourier transform*, IEEE Pulse, viewed 27 October 2019, <https://pulse.embs.org/january-2016/highlights-in-the-history-of-the-fourier-transform/>

[2] National Instruments, *Understanding FFTs and windowing*, National Instruments, viewed 26 October 2019, <http://download.ni.com/evaluation/pxi/Understanding%20FFTs%20and%20Windowing.pdf>

[3] Biological Imaging Faciliity 2009, *Capturing images*, University of California, viewed 1 November 2019, <http://microscopy.berkeley.edu/courses/dib/index.html>

[4] Ottoway, D 2019, *Computer interfacing and fourier analysis practical notes*, Experimental Physics III, University of Adelaide

[5] Cox, B 2018, *Differential equations II course notes*, Differential Equations II, University of Adelaide

[6] Chen, C 2016, *Elements of Human Voice*, World Scientific Publishing, Columbia University